Local Ferroelectricity in $SrTiO_3$ Thin Films

Oleg Tikhomirov
Department of Physics and Astronomy, University of Pittsburgh, 3941 O'Hara Street, Pittsburgh, Pennsylvania 15260
Institute of Solid State Physics, Chernogolovka, Russia 142432

Hua Jiang
Corning Applied Technologies, Woburn, Massachusetts 01801

Jeremy Levy
Department of Physics and Astronomy, University of Pittsburgh, 3941 O'Hara Street, Pittsburgh, Pennsylvania 15260
(Received 4 April 2002; published 10 September 2002)

The temperature-dependent polarization of $SrTiO_3$ thin films is investigated using confocal scanning optical microscopy. A homogeneous out-of-plane and an inhomogeneous in-plane ferroelectric phase are identified from images of the linear electro-optic response. Both hysteretic and nonhysteretic behavior are observed under a dc bias field. Unlike classical transitions in bulk ferroelectrics, local ferroelectricity is observed at temperatures far above the dielectric permittivity maximum. The results demonstrate the utility of local probe experiments in understanding inhomogeneous ferroelectrics.

DOI: 10.1103/PhysRevLett.89.147601 PACS numbers: 77.80.Bh, 77.55.+f

The anomalous properties of strontium titanate ($SrTiO_3$) have resulted in many investigations [1–7]. At high temperatures, the dielectric response exhibits a Curie-Weiss dependence typical for a paraelectric-ferroelectric phase transition, i.e., $\varepsilon_1(T) \propto (T - T_C)^{-1}$, with $T_C \approx 35$ K [4]. However, instead of decreasing below T_C, the permittivity saturates at a high value $\varepsilon_1(0) \approx 24\,000$. This behavior is observed in both pure single crystals [2,3,8] and ceramics [9]. The suppression of a ferroelectric phase transition in $SrTiO_3$ has been attributed to large ground state quantum fluctuations of the soft mode, giving rise to the term "quantum paraelectric" [4,5].

The properties of $SrTiO_3$ are extremely sensitive to dopants and external perturbations. Ferroelectricity can be induced as a result of small concentrations of dopants (Ca, Bi, La…) [10], isotopic substitution in the oxygen octahedra [11], applied electric fields [8], or mechanical pressure [12]. The development of thin film technologies has provided additional ways of controlling structure-sensitive properties. Biaxial strain arising from interaction with a cubic substrate can act as a substitute for external field [13]. Recent calculations predict that thin films of pure $SrTiO_3$, in contrast to bulk materials, should exhibit various ferroelectric and antiferrodistortive phases, depending on the magnitude and sign of the misfit strain [14]. Effects due to inhomogeneous strain are difficult to treat theoretically, although some progress has been made in recent years with first-principles methods [15].

Experimental observation of phase transitions in $SrTiO_3$ thin films is complicated by several factors. Perturbations of cubic $SrTiO_3$ are expected to result in weak or "incipient" ferroelectricity, with narrow hysteresis loops [16]. Inhomogeneous strain arising from relaxation at the film/substrate interface and from other structural defects can make these weak signatures difficult to observe using traditional methods. In these circumstances, spatially resolved techniques are preferable because fluctuating quantities are not averaged out.

Here we report observations of local ferroelectricity in $SrTiO_3$ films, probed by confocal imaging of the linear electro-optic response. $SrTiO_3$ films are grown on $LaAlO_3$ substrates using a metal organic chemical liquid deposition (MOCLD) method. In the MOCLD process, strontium acetate [$Sr(AcO)_2$] and titanium diisopropyl bisacetylacetonate [$TiO\text{-}iPr_2(acac)_2$] were used as precursors. Atomic force microscopic analysis indicated that the surface roughness of the film was around 20 Å. Interdigitated Au/Ti electrodes were fabricated on the top surface by photolithography and liftoff techniques. The thickness of the $SrTiO_3$ film is 800 nm, intermediate Ti layer is 20 nm thick, and electrode itself is 150 nm thick.

The electro-optic response of the $SrTiO_3$ is measured using confocal scanning optical microscopy (CSOM) [17,18]. Light from a HeNe laser is passed through a spatial filter and focused to a diffraction-limited spot on the sample (spot diameter $d \approx 0.5$ μm). A combined dc + ac electric field [$E(t) = E_{dc} + E_{ac}\cos(\Omega t)$, $\Omega/2\pi = 5$ kHz] is applied to interdigitated surface electrodes (gap spacing $L = 25$ μm) to induce an electro-optic modulation of the reflected light. The normalized reflected light is measured with a sensitive balanced photodetector. A lock-in amplifier records the in-phase ($\tilde{I}_{1,\Omega}$) and 90°-shifted ($\tilde{I}_{2,\Omega}$) components of the linear electro-optic response as a function of position (x, y) and bias field E_{dc}. Images of the electro-optic response [$\tilde{I}_{1,\Omega}(x, y)$, $\tilde{I}_{2,\Omega}(x, y)$] are formed by raster scanning the laser beam across the

sample surface. The magnitude of the in-phase signal $|\tilde{I}_{1,\Omega}(x, y)|$ provides a direct signature of ferroelectricity at (x, y). Absence of a linear electro-optic effect $[|\tilde{I}_{1,\Omega}(x, y)| \rightarrow 0]$ indicates either a high symmetry paraelectric phase or specific mutual orientation of ferroelectric axis, electric field, and light polarization canceling the resulting effect of applied electric field on the optical index [17].

Figure 1(a) shows the capacitance, proportional to the dielectric permittivity ε_1, as a function of temperature for the $SrTiO_3$ film and interdigitated structure. In contrast to (Ba, Sr)TiO_3 films [18], $\varepsilon_1(T)$ decreases monotonically over the entire temperature range examined ($100 < T < 300$ K), in accordance with other dielectric investigations [19]. Figures 1(b)–1(e) show CSOM images $[\tilde{I}_{1,\Omega}(x, y)]$ obtained at various temperatures with $E_{dc} = 0$. The high-temperature response [down to $T = 180$ K, Fig. 1(b)] shows $\tilde{I}_{1,\Omega}(x, y) = 0$ over the entire field of view. Small variations are due to shot-noise-limited intensity fluctuations of the laser source, which increase at the metal electrodes due to the high reflectance. As the sample is cooled, areas with pronounced electro-optic response begin to appear. At $T = 164$ K [Fig. 1(c)], $\tilde{I}_{1,\Omega}(x, y)$ is negligibly small in the central region, but is nonzero and uniform near the edges of the electrodes. At $T = 154$ K [Fig. 1(d)], areas between the electrodes start to develop a linear electro-optic response indicative of in-plane ferroelectricity. These signatures grow more pronounced at $T = 146$ K [Fig. 1(d)], showing spatial variations down to the diffraction limit. Distinct regions with $|\tilde{I}_{1,\Omega}(x, y)| = 0$ are observed in some areas of the sample at all temperatures $T > 100$ K.

The field-dependent electro-optic response shows a variety of polarization states in the $SrTiO_3$ film. Examples of observed loops formed by measuring $\tilde{I}_{1,\Omega}(E_{dc})$ at various locations $(x, y)_i$ are presented in Figs. 2(a)–2(c). Both the shape and the amplitude of these local tuning loops vary significantly with location. We observe (a) linear behavior, (b) linear behavior with saturation at high dc bias, and (c) hysteretic curves with high signal at zero bias. In many locations, $\tilde{I}_{1,\Omega}(E_{dc}) = 0$ is found for all E_{dc}, similar to the paraelectric response observed at room temperature $T = 290$ K [Fig. 2(d)].

Ferroelectricity in thin $SrTiO_3$ films was predicted in Ref. [14], and experimental evidence has been reported in Refs. [20]. Different phases, both ferroelectric and nonpolar ones, are predicted depending on the substrate misfit parameter. For the $SrTiO_3/LaAlO_3$ system, there are two competing effects. The lattice constant of $SrTiO_3$ is larger than $LaAlO_3$, so the film is expected to be subject to two-dimensional compression. However, thin films typically relax over a distance ξ that is inversely proportional to the misfit parameter ($\xi \sim 12$ nm for LAO/STO); this relaxation produces misfit dislocations and other defects which can create large local stresses in the film and lead to a spatial distribution of transition-related parameters. A second effect concerns the difference

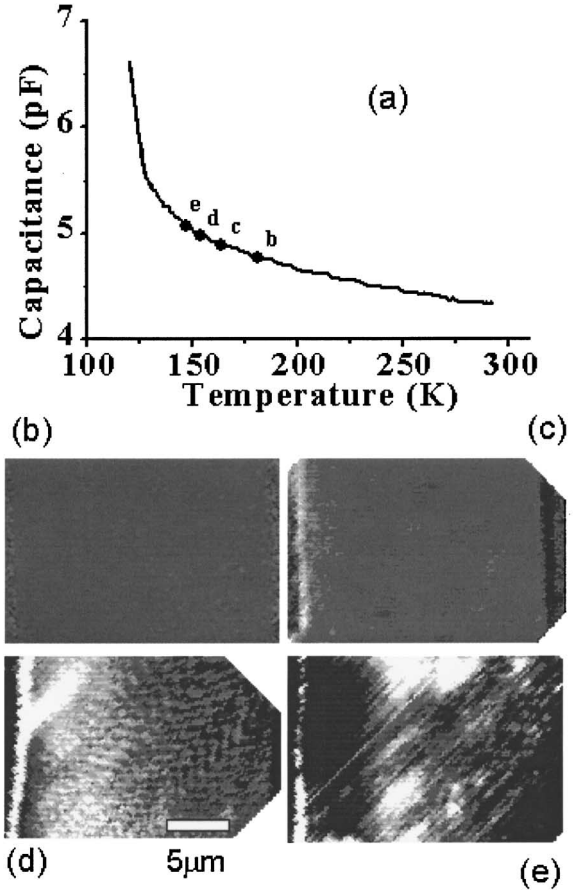

FIG. 1. Phase transition in $SrTiO_3$ thin film. (a) Capacitance vs temperature. (b)–(e) CSOM images taken at $E_{dc} = 0$. (b) $T = 181$ K; (c) $T = 164$ K; (d) $T = 154$ K; (e) $T = 146$ K.

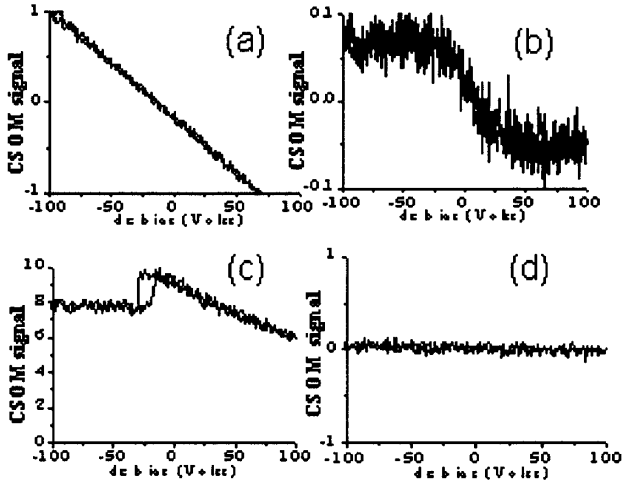

FIG. 2. Examples of local CSOM tuning loops in $SrTiO_3$ thin film. (a) to (c) are measured from different places in the sample at $T = 100$ K; (d) $T = 290$ K.

in thermal expansion coefficients between the film and substrate during cooling. This difference tends to favor tensile expansion of the film. For the relatively thick film considered here (800 nm), we expect the residual compression and thermal mismatch to be comparable in magnitude, leading to an inhomogeneous spatial distribution of dielectric properties.

Observation of areas with linear electro-optic response is consistent with the prediction of ferroelectric ordering in $SrTiO_3$ films. However, the electro-optic images show that the size of ordered regions possessing electro-optic response is small, at or below the diffraction limit, and most likely due to local stresses. The theory developed in Ref. [14] predicts both in-plane and out-of-plane ferroelectric polarization, depending on the magnitude and sign of the in-plane misfit parameter. To identify the predicted phases with observed types of electro-optic response, we must analyze the electro-optic equation [17,18]. The ac electro-optic signal is proportional to the induced change of the absolute value of the optical index $n = \eta^{-1/2}$ in the *local* coordinate system of the optical indicatrix ellipsoid:

$$\Delta\eta = r_{13}E_z(x^2 + y^2) + r_{33}E_z z^2 + r_{42}(E_y yz + E_x xz). \quad (1)$$

Here x, y, and z are the coordinates for an intersection of the light polarization vector with the indicatrix, where by convention, z always coincides with the ferroelectric polarization at a given point. For simplicity, we consider light incident normal to the planar surface. The large relatively field-insensitive values of $|\tilde{I}_{1,\Omega}|$ [Fig. 2(c)] are consistent with in-plane ferroelectric polarization, as depicted in Fig. 3(a). In general, $\tilde{I}_{1,\Omega}$ depends on the relative angle between the polarization and electric field.

The linear field dependence of $\tilde{I}_{1,\Omega}$ [Fig. 2(a)] can be understood by assuming that the ferroelectric polarization is primarily out-of-plane, as depicted in Fig. 3(b). An in-plane bias field E_{dc} deforms the optical indicatrix along the direction of E_{dc} and creates a nonzero contribution due to r_{42} in Eq. (1). For small values of E_{dc} the response is linear, analogous to superparaelectricity or incipient in-plane ferroelectricity. Occasionally, saturated curves are observed [Fig. 2(b)] and are ascribed to completed switching into an in-plane polarization state, or saturation of the polarization. At zero bias, the r_{42} contribution disappears and out-of-plane ferroelectricity no longer contributes to the linear electro-optic response, similar to a proper paraelectric [Fig. 3(c)]. Enhanced signals close to the electrodes [Fig. 1(c)] confirm that the out-of-plane polarization is nonzero. At the electrodes, the perpendicular component of the electric field E_z couples directly to the out-of-plane polarization via r_{33} [Eq. (1)]. The alternating direction at each electrode results in alternating contrast, providing direct evidence that the polarization is uniform in direction.

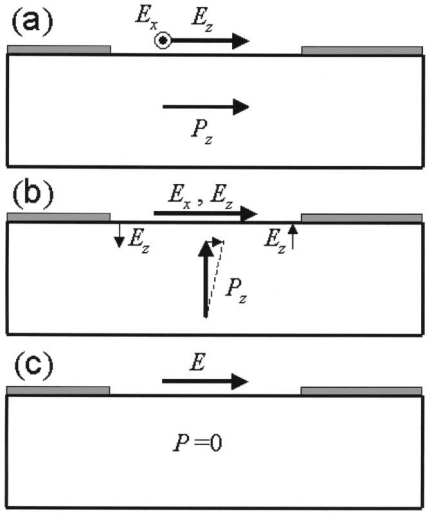

FIG. 3. Possible orientations of local ferroelectric polarization and expected contributions to CSOM response. Schematics depict a cross section of the $SrTiO_3$ film, the ferroelectric polarization vector (P_z), and nonzero components of the electric field produced by the interdigitated top electrodes (E_z, E_x). (a) In-plane ferroelectric polarization; (b) out-of-plane polarization; (c) paraelectric state.

It is remarkable that the observations of local ferroelectricity in $SrTiO_3$ films are not accompanied by corresponding signatures in $\varepsilon_1(T)$. Coexisting regions of paraelectricity and ferroelectricity are observed at temperatures far above the dielectric permittivity maximum. We believe this behavior may help explain some of the peculiar properties of bulk $SrTiO_3$. From permittivity measurements, this material is believed to be quantum paraelectric, obeying the Barrett relation [1]; however, calculations show that quantum fluctuations are not strong enough to prevent ferroelectric displacement completely [4]. Moreover, narrow ferroelectric loops have been reported in pure $SrTiO_3$ samples at low temperature [2,6,11]. One possible explanation is that $SrTiO_3$ below $T = 35$ K is really an incipient ferroelectric with nonzero net polarization, but its dielectric permittivity shows no "classical" decrease below this transition temperature due to a coexistence with virtually paraelectric quantum fluctuations, so the transition is not seen with conventional permittivity measurements.

In summary, we have performed electro-optic imaging of $SrTiO_3$ thin films. The linear electro-optic response confirms the existence of ferroelectricity at low temperature. Spatial distribution of the ferroelectric phase is likely driven by inhomogeneous stress. Local field-dependent experiments show both hysteretic and nonhysteretic behavior. It was shown that ferroelectricity in $SrTiO_3$ thin films is not accompanied by a corresponding signature in the dielectric permittivity, as it is in bulk materials.

This work was supported by the Office of Naval Research (N00173-98-1-G011) and the National Science Foundation (DMR-9701725).

[1] J. H. Barrett, Phys. Rev. **86**, 118 (1952).
[2] H. E. Weaver, J. Phys. Chem. Solids **11**, 274 (1959).
[3] R. C. Neville, B. Hoeneisen, and C. A. Mead, J. Appl. Phys. **43**, 2124 (1972).
[4] K. A. Muller and H. Bukard, Phys. Rev. B **19**, 3593 (1979).
[5] K. A. Muller, W. Berlinger, and E. Tosatti, Z. Phys. B **84**, 277 (1991).
[6] J. Hemberger *et al.*, Phys. Rev. B **52**, 13159 (1995).
[7] J. F. Scott, A. Chen, and H. Ledbetter, J. Phys. Chem. Solids **61**, 185 (2000).
[8] E. Hegenbarth, Phys. Status Solidi **6**, 333 (1964).
[9] J. K. Hulm, Proc. Phys. Soc. London Sect. A **63**, 1184 (1950).
[10] T. Mitsui and W. B. Westphal, Phys. Rev. **124**, 1354 (1961).
[11] M. Itoh *et al.*, Phys. Rev. Lett. **82**, 3540 (1999).
[12] W. J. Burke and R. J. Pressley, Solid State Commun. **9**, 191 (1971); H. Uwe and T. Sakudo, Phys. Rev. B **13**, 271 (1976).
[13] J. S. Speck *et al.*, J. Appl. Phys. **76**, 477 (1994); N. A. Pertsev, A. G. Zembilgotov, and A. K. Tagantsev, Phys. Rev. Lett. **80**, 1988 (1998).
[14] N. A. Pertsev, A. K. Tagantsev, and N. Setter, Phys. Rev. B **61**, R825 (2000).
[15] L. Bellaiche, A. Garcia, and D. Vanderbilt, Phys. Rev. Lett. **84**, 5427 (2000).
[16] H. E. Weaver, J. Phys. Chem. Solids **11**, 274 (1959).
[17] O. Tikhomirov *et al.*, J. Appl. Phys. **87**, 1932 (2000).
[18] O. Tikhomirov and J. Levy, Appl. Phys. Lett. **77**, 2048 (2000).
[19] K. C. Park and J. H. Cho, Appl. Phys. Lett. **77**, 435 (2000); M. Lippmaa *et al.*, Appl. Phys. Lett. **74**, 3543 (1999); A. Chen *et al.*, Appl. Phys. Lett. **78**, 2754 (2001).
[20] D. Fuchs *et al.*, J. Appl. Phys. **85**, 7362 (1999); A. A. Sirenko *et al.*, Phys. Rev. Lett. **82**, 4500 (1999).